

Interaction of Lamb modes with two-level systems in amorphous nanoscopic membranes

T. Kühn,¹ D. V. Anghel,^{2,3} Y. M. Galperin,^{4,5,6} and M. Manninen¹¹*Nanoscience Center, Department of Physics, University of Jyväskylä, P.O. Box 35, FIN-40014 University of Jyväskylä, Finland*²*Department of Theoretical Physics, National Institute for Physics and Nuclear Engineering-“Horia Hulubei”, Strada Atomistilor No. 407, P.O. Box MG-6, 077125 Bucharest-Magurele, Romania*³*Bogoliubov Laboratory of Theoretical Physics, JINR, Dubna 141980, Russia*⁴*Department of Physics and Centre of Advanced Materials and Nanotechnology, University of Oslo, P.O. Box 1048 Blindern, 0316 Oslo, Norway*⁵*Argonne National Laboratory, 9700 S. Cass Avenue, Argonne, Illinois 60439, USA*⁶*A. F. Ioffe Physico-Technical Institute of Russian Academy of Sciences, 194021 St. Petersburg, Russia*

(Received 14 May 2007; published 23 October 2007)

Using a generalized model of interaction between a two-level system (TLS) and an arbitrary deformation of the material, we calculate the interaction of Lamb modes with TLSs in amorphous nanoscopic membranes. We compare the mean free paths of the Lamb modes of different symmetries and calculate the heat conductivity κ . In the limit of an infinitely wide membrane, the heat conductivity is divergent. Nevertheless, the finite size of the membrane imposes a lower cutoff for the phonon frequencies, which leads to the temperature dependence $\kappa \propto T(a+b \ln T)$. This temperature dependence is a hallmark of the TLS-limited heat conductance at low temperature.

DOI: 10.1103/PhysRevB.76.165425

PACS number(s): 68.60.-p, 65.60.+a

I. INTRODUCTION

The development of nanodetectors and the strict requirements on their performance triggered intense experimental and theoretical studies of their thermal properties. These detectors work usually in a temperature range around 1 K or below, and are supported by thin, insulating membranes. The thickness of such membranes is of the order of 100 nm, which, in the given temperature range, makes it comparable to the dominant thermal phonon wavelength. In problems where the phonon wavelength is comparable to or longer than some of the dimensions of the system in question, the three-dimensional phonon gas model cannot be applied anymore to calculate the system's thermal properties. Instead, one has to use the phonon modes specific to the system. If, like in our case at subkelvin temperatures, the mean free path is much longer than the wavelength, these phonon modes are the eigenmodes of the elastic equation for the given geometry.

The membranes that support the detectors are made of amorphous, low stress silicon nitride (SiN_x) and their thermal properties have been measured in various geometries by different groups (see, for example, Refs. 1–6). Depending on the quality and the dimensions of the samples, and possibly the temperature range in which measurements were done, the heat flux along the membrane may be due to either diffusive^{2–4,7} or radiative phonon transport.^{3,5} In the case of diffusive phonon transport, it was observed that the heat conductivity κ is roughly proportional to T^2 .

For a better thermal insulation of the detector, the underlying membrane is sometimes cut. The result is a self-supporting structure with a wider area in the middle, connected to the bulk by long, narrow bridges, like in Fig. 1(b).^{1,2} The heat conductivity along such bridges has again a power law dependence on the temperature, $\kappa \propto T^p$, where p takes values between 1.5 and 2.^{1,2} For the samples measured

in Ref. 2, p increased with the width of the bridge.

The heat capacity of a membrane is more difficult to measure directly since the membrane is always in contact with the bulk. However, it can be estimated by applying ac heating and measuring the amplitude of the temperature oscillations. In this way, Leivo and Pekola² observed that the ratio c_V/κ , where c_V is the heat capacity, increases with temperature for the narrowest bridges.

As mentioned above, to explain theoretically all these observations, we have to work with the proper set of phonon modes. For wide membranes with parallel surfaces, the eigenmodes of the elastic equations are called *Lamb modes* and *horizontal shear modes*, as explained, for example, in Ref. 8. Using these modes and their dispersion relations, we could describe quite well the thermal properties of the membranes in the low temperature limit,⁹ i.e., at temperatures where the characteristic thermal wavelength of the phonons is much longer than the thickness of the membrane. For a typical 100 nm thick SiN_x membrane, the characteristic thermal wavelength becomes larger than the membrane thickness at about 250 mK.

Nevertheless, the same temperature dependence of the heat conductivity and heat capacity persists also in a temperature range where this characteristic thermal wavelength becomes equal to or even smaller than the thickness. This can no longer be explained only by the dispersion relation of the Lamb modes in the membrane, and we have to take into account the amorphous structure of the membrane and the resulting phonon scattering.

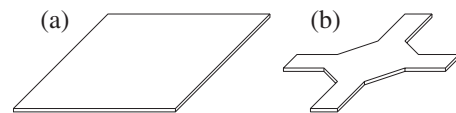


FIG. 1. (a) Full, dielectric membrane. (b) Cut membrane for better thermal insulation.

An amorphous material contains dynamic defects which can be modeled by an ensemble of two-level systems (TLSs).^{10–12} A TLS can be understood as an atom or group of atoms which can tunnel between two close minima in the configuration space. Any deformation of the material disturbs the TLS, which can have a transition (an excitation or a deexcitation) to the other energy level. A passing phonon produces such a deformation and, therefore, may be scattered by the TLS. In bulk materials, the phonon modes are simple, transversally or longitudinally polarized plane waves, and the deformation field they produce can be described by only two parameters, the wave vector (or the wavelength) and the polarization. As a consequence, in the so-called *standard tunneling model*, the interaction Hamiltonian has a very simple structure.^{10–12} In a mesoscopic system, the deformation caused by the *displacement field* of a phonon mode is more complex and the TLS-phonon interaction Hamiltonian has to be modified accordingly. This was done in Ref. 13. Here, we use this more general Hamiltonian to calculate the interaction of the phonon modes of the membrane with the TLSs.

II. TWO-LEVEL SYSTEM-PHONON INTERACTION

A TLS is described by a Hamiltonian which has the form

$$H_{\text{TLS}} = \frac{\Delta}{2}\sigma_z - \frac{\Lambda}{2}\sigma_x \quad (1)$$

when written in the basis formed by the ground states of the two potential wells between which the system tunnels.¹³ In Eq. (1), Δ is the *asymmetry of the potential*, Λ is the *tunnel splitting*, and σ_x , σ_z are Pauli matrices. The Hamiltonian (1) can be diagonalized by an orthogonal transformation O ,

$$H'_{\text{TLS}} \equiv O^T H_{\text{TLS}} O = \frac{\epsilon}{2}\sigma_z, \quad (2)$$

and we obtain the excitation energy, $\epsilon \equiv \sqrt{\Delta^2 + \Lambda^2}$. Everywhere in this paper the superscript T denotes the *transpose* of a matrix.

The TLS parameters Δ and Λ are not the same for all the TLSs in the material, but they are well modeled by the distribution $P(\Lambda, \Delta) = P_0/\Lambda$ in the unit volume of the material. We can rewrite the function P in terms of the more practical variables ϵ and $u \equiv \Lambda/\epsilon$,

$$P(\epsilon, u) = \frac{P_0}{u\sqrt{1-u^2}}. \quad (3)$$

The TLSs that have an excitation energy comparable to $k_B T$ are very efficient phonon scatterers.

The deformation due to the displacement field of a phonon is quantitatively described by the *strain field*, which will be represented here by the six-component vector \mathbf{S} .⁸ If we denote the displacement field by $\mathbf{u}(\mathbf{r})$, then the strain is defined as the *symmetric gradient* of $\mathbf{u}(\mathbf{r})$, i.e., $\mathbf{S}^T \equiv (\nabla_S \mathbf{u})^T = (\partial_x u_x, \partial_y u_y, \partial_z u_z, \partial_y u_z + \partial_z u_y, \partial_x u_z + \partial_z u_x, \partial_x u_y + \partial_y u_x)$. This deformation adds a time-dependent perturbation to the Hamiltonian (1), which we shall denote by H_1 . The perturbation is

assumed to be diagonal when written in the basis of the two ground states of the potential wells [like in Eq. (1)],^{10–12,14,15}

$$H_1 = \frac{\delta}{2}\sigma_z, \quad (4)$$

and linear in the strain field at the location of the TLS,^{13,15}

$$\delta = 2\tilde{\gamma} \mathbf{T}^t \cdot [\mathbf{r}] \cdot \mathbf{S}. \quad (5)$$

The other quantities in Eq. (5) are the *coupling constant* $\tilde{\gamma}$, the six-component vector \mathbf{T} , which is defined by a generic orientation $\hat{\mathbf{t}}$ of the TLS as $\mathbf{T} \equiv (t_x^2, t_y^2, t_z^2, 2t_y t_z, 2t_x t_z, 2t_x t_y)^T$, and the 6×6 matrix of the deformation potential parameters $[\mathbf{r}]$. For isotropic materials, the matrix $[\mathbf{r}]$ is

$$[\mathbf{r}] = \begin{pmatrix} 1 & \zeta & \zeta & 0 & 0 & 0 \\ \zeta & 1 & \zeta & 0 & 0 & 0 \\ \zeta & \zeta & 1 & 0 & 0 & 0 \\ 0 & 0 & 0 & \xi & 0 & 0 \\ 0 & 0 & 0 & 0 & \xi & 0 \\ 0 & 0 & 0 & 0 & 0 & \xi \end{pmatrix}, \quad (6)$$

with the TLS potential parameters ξ and ζ that satisfy the condition $\zeta + 2\xi = 1$.¹³

To calculate the scattering probabilities, we have to write H_1 in the second quantization. For this, we denote the TLS excited state by $|\uparrow\rangle$ and its ground state by $|\downarrow\rangle$, and we introduce the “creation” and “annihilation” operators a^\dagger and a , respectively, so that $a^\dagger|\downarrow\rangle = |\uparrow\rangle$, $a|\uparrow\rangle = |\downarrow\rangle$, $a^\dagger|\uparrow\rangle = 0$, and $a|\downarrow\rangle = 0$. The operators a and a^\dagger obey Fermi commutation relations, and in matrix form, we have $\sigma_z = (2a^\dagger a - 1)$ and $\sigma_x = (a^\dagger + a)$. The bosonic creation and annihilation operators for phonons will be denoted by b_μ^\dagger and b_μ , respectively, where μ stands, in general, for the quantum numbers of the phonon modes (see, for example, Refs. 13–16). Using these notations and applying the transformation O to the total Hamiltonian $[O^T(H_{\text{TLS}} + H_1)O \equiv H'_{\text{TLS}} + H'_1]$, we obtain

$$H'_1 = \frac{\tilde{\gamma}\Delta}{\epsilon} \mathbf{T}^T \cdot [\mathbf{r}] \cdot \sum_{\mu} [\mathbf{S}_{\mu} b_{\mu} + \mathbf{S}_{\mu}^* b_{\mu}^{\dagger}] (2a^{\dagger} a - 1) - \frac{\tilde{\gamma}\Lambda}{\epsilon} \mathbf{T}^T \cdot [\mathbf{r}] \cdot \sum_{\mu} [\mathbf{S}_{\mu} b_{\mu} + \mathbf{S}_{\mu}^* b_{\mu}^{\dagger}] (a^{\dagger} + a). \quad (7)$$

In the first order perturbation theory, the phonon absorption and emission rates are determined by the off-diagonal elements of H'_1 , i.e., of the second row of Eq. (7). Higher order processes are not considered here.

Phonon modes in the membrane

The phonon modes of a freestanding, infinite membrane are divided into three groups, according to their symmetry properties. One group is formed of simple, transversally polarized modes, called the horizontal shear modes (h). The two other groups are the symmetric (s) and antisymmetric (a) Lamb modes. Together, these modes form a complete, orthonormal set of functions for the elastic displacement fields in the membrane, and their proper quantization has

been carried out in Ref. 16. In this paper, we shall use the results and notations from there, and we shall call the three different types of phonons (i.e., h , s , and a) *polarizations*.

We assume that the membrane of thickness d is placed parallel to the (xy) plane and its parallel surfaces cut the z axis at $\pm d/2$. The phonons propagate in the (xy) plane with the wave vector $\mathbf{k}_{\parallel} = k_{\parallel} \hat{\mathbf{k}}_{\parallel}$, of real k_{\parallel} . We use a *hat* to denote unit vectors.

Along the z direction, the phonon modes are stationary. As the h modes are pure transversal waves, they have only one wave vector component along the z direction, which we denote by k_h . The s and a waves are superpositions of transversal and longitudinal waves of wave vector components along the z direction denoted by k_t and k_l , respectively. Due to the boundary conditions, which demand that the membrane surfaces are stress-free, k_h takes the discrete values $m\pi/d$, with m taking all integer values between 0 and ∞ , whereas k_t and k_l satisfy the more complicated relations⁸

$$\frac{\tan(k_t d/2)}{\tan(k_l d/2)} = -\frac{4k_t k_l k_{\parallel}^2}{(k_t^2 - k_{\parallel}^2)^2} \quad (8a)$$

for the symmetric modes and

$$\frac{\tan(k_t d/2)}{\tan(k_l d/2)} = -\frac{4k_t k_l k_{\parallel}^2}{(k_t^2 - k_{\parallel}^2)^2} \quad (8b)$$

for the antisymmetric modes. Equations (8a) and (8b) plus Snell's law, $\omega^2 = c_t^2(k_{\parallel}^2 + k_t^2) = c_l^2(k_{\parallel}^2 + k_l^2)$, enable us to write k_t , as a function of k_l for each of the polarizations s and a . (In Snell's law, c_t and c_l are the respective transversal and longitudinal sound velocities for bulk media.) Like in the case of the h modes, the dispersion relations for the symmetric and antisymmetric modes split into branches, i.e., Eqs. (8a) and (8b) and Snell's law do not give only one function $k_t(k_l)$ for either set of modes, but produce an infinite, countable set of such functions. These functions will be called *phonon branches* and we shall number them with $m=0, 1, \dots$, as we did in Ref. 16, where branches of bigger m lie above branches of smaller m in the (k_l, k_t) plane.

A simple way to express the quantum numbers of the phonon modes is to use Eqs. (8a) and (8b) and Snell's law to write the functions $k_t(k_{\parallel})$ and $k_l(k_{\parallel})$. Then each branch of polarization $\sigma=s, a$ and branch number m is going to be described by the continuous set of numbers $[k_t(k_{\parallel}), k_l(k_{\parallel})]_{\sigma, m}$, with k_{\parallel} taking values from 0 to ∞ . We, therefore, choose the set μ of quantum numbers that specify the phonon modes in Eq. (7) to be $\mu \equiv \{\sigma, m, \mathbf{k}_{\parallel}\}$.

The functions $k_t(k_{\parallel})$ and $k_l(k_{\parallel})$ may take both real and imaginary values. To distinguish between these situations, we write the imaginary values of k_t as $i\kappa_t$ and the imaginary values of k_l as $i\kappa_l$. In these notations, $k_{t,t}$ and $\kappa_{l,t}$ take always positive, real values.

In order to simplify the later discussion, we shall replace k_t and k_l with the complex quantities $\bar{k}_t \equiv k_t + i\kappa_t$ and $\bar{k}_l \equiv k_l + i\kappa_l$, respectively. Note, however, that \bar{k}_t and \bar{k}_l are never really complex, but they are *either* real *or* imaginary, as long as k_{\parallel} is real.¹⁶

The displacement fields of the phonon modes are^{8,16}

$$\mathbf{u}_h = N_h \cos[k_h(z - d/2)] (\hat{\mathbf{k}}_{\parallel} \times \hat{\mathbf{z}}) e^{i(\mathbf{k}_{\parallel} \cdot \mathbf{r} - \omega t)}, \quad (9a)$$

$$\begin{aligned} \mathbf{u}_s = N_s \{ & i\bar{k}_t [2k_{\parallel}^2 \cos(\bar{k}_t d/2) \cos(\bar{k}_l z) + [\bar{k}_t^2 - k_{\parallel}^2] \cos(\bar{k}_l d/2) \\ & \times \cos(\bar{k}_t z)] \hat{\mathbf{k}}_{\parallel} - k_{\parallel} [2\bar{k}_t \bar{k}_l \cos(\bar{k}_t d/2) \sin(\bar{k}_l z) - [\bar{k}_t^2 \\ & - k_{\parallel}^2] \cos(\bar{k}_l d/2) \sin(\bar{k}_t z)] \hat{\mathbf{z}} \} e^{i(\mathbf{k}_{\parallel} \cdot \mathbf{r} - \omega t)}, \end{aligned} \quad (9b)$$

$$\begin{aligned} \mathbf{u}_a = N_a \{ & i\bar{k}_t [2k_{\parallel}^2 \sin(\bar{k}_t d/2) \sin(\bar{k}_l z) + [\bar{k}_t^2 - k_{\parallel}^2] \sin(\bar{k}_l d/2) \\ & \times \sin(\bar{k}_t z)] \hat{\mathbf{k}}_{\parallel} + k_{\parallel} [2\bar{k}_t \bar{k}_l \sin(\bar{k}_t d/2) \cos(\bar{k}_l z) - [\bar{k}_t^2 \\ & - k_{\parallel}^2] \sin(\bar{k}_l d/2) \cos(\bar{k}_t z)] \hat{\mathbf{z}} \} e^{i(\mathbf{k}_{\parallel} \cdot \mathbf{r} - \omega t)}. \end{aligned} \quad (9c)$$

As one can see, when \bar{k}_t or \bar{k}_l take imaginary values, the trigonometric functions in Eq. (9) will switch into hyperbolic functions. The normalization constants N_h , N_s , and N_a are given by¹⁶

$$N_h^{-2} = \begin{cases} V, & m=0 \\ V/2, & m>0, \end{cases} \quad (10a)$$

$$\begin{aligned} N_s^{-2} = A \left\{ & 4|\bar{k}_t|^2 k_{\parallel}^2 \left| \cos\left(\frac{\bar{k}_t d}{2}\right) \right|^2 \left((|\bar{k}_l|^2 + k_{\parallel}^2) \frac{\sinh(\kappa_l d)}{2\kappa_l} - (|\bar{k}_l|^2 - k_{\parallel}^2) \frac{\sin(k_l d)}{2k_l} \right) + |\bar{k}_t^2 - k_{\parallel}^2|^2 \left| \cos\left(\frac{\bar{k}_l d}{2}\right) \right|^2 \right. \\ & \left. \times \left((|\bar{k}_t|^2 + k_{\parallel}^2) \frac{\sinh(\kappa_t d)}{2\kappa_t} + (|\bar{k}_t|^2 - k_{\parallel}^2) \frac{\sin(k_t d)}{2k_t} \right) - 4k_{\parallel}^2 \left| \cos\left(\frac{\bar{k}_t d}{2}\right) \right|^2 \left[\kappa_t (|\bar{k}_t|^2 + k_{\parallel}^2) \sinh(\kappa_t d) - k_t (|\bar{k}_t|^2 - k_{\parallel}^2) \sin(k_t d) \right] \right\}, \end{aligned} \quad (10b)$$

$$\begin{aligned} N_a^{-2} = A \left\{ & 4|\bar{k}_t|^2 k_{\parallel}^2 \left| \sin\left(\frac{\bar{k}_t d}{2}\right) \right|^2 \left((|\bar{k}_l|^2 + k_{\parallel}^2) \frac{\sinh(\kappa_l d)}{2\kappa_l} + (|\bar{k}_l|^2 - k_{\parallel}^2) \frac{\sin(k_l d)}{2k_l} \right) + |\bar{k}_t^2 - k_{\parallel}^2|^2 \left| \sin\left(\frac{\bar{k}_l d}{2}\right) \right|^2 \right. \\ & \left. \times \left((|\bar{k}_t|^2 + k_{\parallel}^2) \frac{\sinh(\kappa_t d)}{2\kappa_t} - (|\bar{k}_t|^2 - k_{\parallel}^2) \frac{\sin(k_t d)}{2k_t} \right) - 4k_{\parallel}^2 \left| \sin\left(\frac{\bar{k}_t d}{2}\right) \right|^2 \left[\kappa_t (|\bar{k}_t|^2 + k_{\parallel}^2) \sinh(\kappa_t d) + k_t (|\bar{k}_t|^2 - k_{\parallel}^2) \sin(k_t d) \right] \right\}, \end{aligned} \quad (10c)$$

where A is the area of the membrane and $V=dA$ is its volume. To obtain the expressions for N_s and N_a for the different combinations of real or imaginary \bar{k}_t and \bar{k}_l , one has to *take the limit to 0* of their redundant components in Eqs. (10b) and (10c). For example, if \bar{k}_t is real and \bar{k}_l is imaginary, we calculate the corresponding normalization factor by taking in Eq. (10b) or (10c) the limits $\kappa_t \rightarrow 0$ and $k_l \rightarrow 0$.¹⁶

III. TRANSITION RATES

Now we have all the ingredients to calculate the TLS transition rates or phonon absorption and emission probabilities.

We shall denote the phonon-TLS quantum states by $|n_\mu, \downarrow\rangle$ or $|n_\mu, \uparrow\rangle$, where we denoted the number of phonons on the mode μ by n_μ . Using Eq. (7), we write the emission amplitude of a phonon by a TLS as

$$\langle n_\mu, \uparrow | \tilde{H}_1 | n_\mu + 1, \downarrow \rangle = -\frac{\tilde{\gamma}\Lambda}{\epsilon} \sqrt{\frac{\hbar n_\mu}{2\rho\omega_\mu}} M_\mu^*, \quad (11)$$

with M_μ is given by

$$M_\mu(\hat{\mathbf{t}}) = \mathbf{T}^T \cdot [r] \cdot \mathbf{S}_\mu.$$

Explicitly, for the three phonon polarizations, we have

$$M_{h,m,k_\parallel}(\hat{\mathbf{t}}) = 2\xi N_h \{ -t_y t_z k_h \sin[k_h(z-d/2)] + it_x t_y k_\parallel \cos[k_h(z+d/2)] \} e^{ik_\parallel x}, \quad (12a)$$

$$\begin{aligned} M_{s,m,k_\parallel}(\hat{\mathbf{t}}) = N_s \{ & -2\bar{k}_t k_\parallel \cos(\bar{k}_t d/2) \cos(\bar{k}_t z) \{ k_\parallel^2 [\zeta + (1-\zeta)t_x^2] + \bar{k}_t^2 [\zeta + (1-\zeta)t_z^2] \} + \bar{k}_t k_\parallel [\bar{k}_t^2 - k_\parallel^2] \cos(\bar{k}_t d/2) \cos(\bar{k}_t z) (\zeta - 1) (t_x^2 - t_z^2) \\ & - 8it_x t_z \xi \bar{k}_t \bar{k}_l k_\parallel^2 \cos(\bar{k}_t d/2) \sin(\bar{k}_t z) - 2it_x t_z \xi [\bar{k}_t^2 - k_\parallel^2]^2 \cos(\bar{k}_t d/2) \sin(\bar{k}_t z) \} \end{aligned} \quad (12b)$$

$$\begin{aligned} M_{a,m,k_\parallel}(\hat{\mathbf{t}}) = N_a \{ & -2\bar{k}_t k_\parallel \sin(\bar{k}_t d/2) \sin(\bar{k}_t z) \{ k_\parallel^2 [t_x^2 + \zeta(1-t_x^2)] + \bar{k}_t^2 [t_z^2 + \zeta(1-t_z^2)] \} - k_\parallel \bar{k}_t [\bar{k}_t^2 - k_\parallel^2] \sin(\bar{k}_t d/2) \sin(\bar{k}_t z) (1-\zeta) (t_x^2 - t_z^2) \\ & + 8it_x t_z \xi \bar{k}_t \bar{k}_l k_\parallel^2 \sin(\bar{k}_t d/2) \cos(\bar{k}_t z) + 2t_x t_z \xi [\bar{k}_t^2 - k_\parallel^2]^2 \sin(\bar{k}_t d/2) \cos(\bar{k}_t z) \}, \end{aligned} \quad (12c)$$

where k_t and k_l are implicitly determined by the branch number m and k_\parallel . Using Fermi's golden rule, we calculate the phonon absorption and emission rates Γ_{abs}^μ and Γ_{em}^μ , respectively,

$$\Gamma_{\text{abs}}^\mu = \frac{\pi}{\rho\omega_\mu} \frac{\tilde{\gamma}^2 \Lambda^2}{\epsilon^2} |M_\mu|^2 n_\mu \delta(\hbar\omega_\mu - \epsilon), \quad (13a)$$

$$\Gamma_{\text{em}}^\mu = \frac{\pi}{\rho\omega_\mu} \frac{\tilde{\gamma}^2 \Lambda^2}{\epsilon^2} |M_\mu|^2 (n_\mu + 1) \delta(\hbar\omega_\mu - \epsilon), \quad (13b)$$

where ϵ is the energy of the TLS, as defined in Sec. II, and ω is the angular frequency of the phonon.

In an amorphous solid, the orientations of the TLSs are arbitrary, so the relevant quantities for our calculations are the averages of Γ_{abs}^μ over the directions $\hat{\mathbf{t}}$ of the TLSs. The only quantity that depends on $\hat{\mathbf{t}}$ in Eqs. (13) is $|M_\mu|^2$. Additionally, we assume that the distribution of TLSs in the membrane is uniform, which leaves again $|M_\mu|^2$, the only quantity dependent on z in the expressions, for the absorption and emission rates. As we are interested in an average scattering probability rather than in a detailed description of where along the z direction the scattering takes place, we also average $|M_\mu|^2$ along z . Denoting by $\langle \cdot \rangle$ the average over the TLS orientations and the z variable, we obtain

$$\langle |M_h|^2 \rangle = \frac{C_t}{V} (k_\parallel^2 + k_h^2), \quad (14a)$$

$$\begin{aligned} \langle |M_s|^2 \rangle = \frac{N_s}{d} \left\{ & 4C_l |\bar{k}_t|^2 k_\parallel^2 k_t^2 + \bar{k}_t^2 \left| \cos\left(\frac{\bar{k}_t d}{2}\right) \right|^2 \left(\frac{\sinh(\kappa_t d)}{2\kappa_t} + \frac{\sin(k_l d)}{2k_l} \right) + C_t |\bar{k}_t^2 - k_\parallel^2|^2 \left| \cos\left(\frac{\bar{k}_t d}{2}\right) \right|^2 \right. \\ & \times \left((|\bar{k}_t|^2 + k_\parallel^2)^2 \frac{\sinh(\kappa_t d)}{2\kappa_t} - (|\bar{k}_t|^2 - k_\parallel^2)^2 \frac{\sin(k_l d)}{2k_l} \right) - 2C_t k_t (2k_\parallel^6 - k_\parallel^4 |\bar{k}_t|^2 - |\bar{k}_t|^6) \left| \cos\left(\frac{\bar{k}_t d}{2}\right) \right|^2 \\ & \left. \times \sin(k_l d) - 2C_t \kappa_t (2k_\parallel^6 + k_\parallel^4 |\bar{k}_t|^2 + |\bar{k}_t|^6) \left| \cos\left(\frac{\bar{k}_t d}{2}\right) \right|^2 \sinh(\kappa_t d) \right\}, \end{aligned} \quad (14b)$$

$$\begin{aligned}
 \langle |M_d|^2 \rangle = & \frac{N^2}{d} \left\{ 4C_l |\bar{k}_l|^2 k_\parallel^2 |k_\parallel^2 + \bar{k}_l^2|^2 \left| \sin\left(\frac{\bar{k}_l d}{2}\right) \right|^2 \left(\frac{\sinh(\kappa_l d)}{2\kappa_l} - \frac{\sin(k_l d)}{2k_l} \right) + C_l |\bar{k}_l^2 - k_\parallel^2|^2 \left| \sin\left(\frac{\bar{k}_l d}{2}\right) \right|^2 \right. \\
 & \times \left((|\bar{k}_l|^2 + k_\parallel^2) \frac{\sinh(\kappa_l d)}{2\kappa_l} + (|\bar{k}_l|^2 - k_\parallel^2) \frac{\sin(k_l d)}{2k_l} \right) - 2C_l k_l (-2k_\parallel^6 + k_\parallel^4 |\bar{k}_l|^2 + |\bar{k}_l|^6) \left| \sin\left(\frac{\bar{k}_l d}{2}\right) \right|^2 \\
 & \left. \times \sin(k_l d) - 2C_l \kappa_l (2k_\parallel^6 + k_\parallel^4 |\bar{k}_l|^2 + |\bar{k}_l|^6) \left| \sin\left(\frac{\bar{k}_l d}{2}\right) \right|^2 \sinh(\kappa_l d) \right\}. \quad (14c)
 \end{aligned}$$

C_l and C_t are constants that depend on the deformation potential parameter ξ , $C_l = 4\xi^2/15$ and $C_t = (15 - 40\xi + 32\xi^2)/15$. Note that $C_l > C_t \geq 0$ for all ξ .¹³ Using Eqs. (13) and (14), we can calculate the TLS and phonon relaxation times,

$$\tau_\epsilon^{-1} = \frac{\pi \tilde{\gamma}^2 \Lambda^2}{\rho \epsilon^2} \coth\left(\frac{\beta\epsilon}{2}\right) \sum_\mu \frac{1}{\omega_\mu} \langle |M_\mu|^2 \rangle \delta(\hbar\omega_\mu - \epsilon) \quad (15)$$

and

$$\begin{aligned}
 \tau_\mu^{-1} &= \frac{\pi \tilde{\gamma}^2}{\rho \omega_\mu \epsilon_{,u}} \sum u^2 \langle |M_\mu|^2 \rangle \tanh\left(\frac{\beta\epsilon}{2}\right) \delta(\hbar\omega_\mu - \epsilon) \\
 &= \frac{\pi \tilde{\gamma}^2 V P_0}{\rho \omega_\mu} \langle |M_\mu|^2 \rangle \tanh\left(\frac{\beta\hbar\omega}{2}\right), \quad (16)
 \end{aligned}$$

respectively. Here, we changed the summation over u and ϵ into a two-dimensional integral and used the TLS density (3).

Using Eq. (16), we can calculate the two-dimensional heat conductivity along the membrane,

$$\begin{aligned}
 \kappa &= \frac{1}{A} \sum_\mu \hbar \omega_\mu \tau_\mu (v_\mu)_x^2 \frac{\partial n_\mu}{\partial T} \\
 &= \frac{\hbar^2 \rho}{16\pi^2 \tilde{\gamma}^2 V P_0 k_B T^2} \sum_{n,\sigma} \int_0^\infty dk_\parallel \left(\frac{\partial \omega_{n,\sigma}}{\partial k_\parallel} \right)^2 \frac{k_\parallel \omega_{n,\sigma}^3}{\langle |M_{n,\sigma}|^2 \rangle} \\
 &\quad \times \frac{\coth(\beta\hbar\omega_{n,\sigma}/2)}{\sinh^2(\beta\hbar\omega_{n,\sigma}/2)}. \quad (17)
 \end{aligned}$$

For the last expression, we wrote explicitly $\mu = (n, \sigma, k_\parallel)$ and converted the summation over k_\parallel into an integral, omitting the k_\parallel dependence of ω and $|M|^2$ for brevity. At an arbitrary temperature, κ has to be calculated numerically. In this paper, we give only the analytical low temperature approximation.

IV. LOW ENERGY EXPANSION: ASYMPTOTIC RESULTS

We can analytically calculate the scattering times or the thermal properties of the membrane only in the long-wavelength limit, i.e., for the branch $m=0$ for each of the three polarizations of the phonon modes and $k_\parallel \ll 1/d$. The calculation of thermal properties in this limit corresponds to a temperature range in which $k_B T \ll \hbar c_l/d$. First, we have to calculate the relaxation times for each polarization.

A. h mode

For the lowest branch of the h mode, $\omega_{h,0}$ is linear in k_\parallel , and using Eq. (14a), the calculation of $\tau_{h,0,k_\parallel(\omega)}$ is straightforward for any ω ,

$$\tau_{h,0,k_\parallel(\omega)} = \frac{\hbar \rho c_t^2}{\pi \tilde{\gamma}^2 P_0 C_t} \frac{1}{\hbar \omega} \coth(\beta\hbar\omega/2). \quad (18)$$

B. s mode

To get a long-wavelength expression of the dispersion relation for the lowest branch of the s mode, we note that $\bar{k}_l = i\kappa_l$ takes imaginary values, which turns Eq. (8a) into

$$\frac{\tan(k_l b/2)}{\tanh(\kappa_l b/2)} = \frac{4k_l \kappa_l k_\parallel^2}{(k_l^2 - \kappa_l^2)^2}. \quad (19)$$

We expand the trigonometric functions in Eq. (19) to leading order and obtain

$$\omega_{s,0,k_\parallel} = 2 \frac{c_t}{c_l} \sqrt{c_l^2 - c_t^2} k_\parallel \equiv c_s k_\parallel. \quad (20)$$

Using this, we calculate the relaxation time for this branch,

$$\begin{aligned}
 \tau_{s,0,k_\parallel(\omega)} &= \frac{\hbar \rho c_t^2}{\pi \tilde{\gamma}^2 P_0 C_t c_l^4 + C_t c_l^2 (c_l^2 - 2c_t^2)} \frac{4c_l^2 (c_l^2 - c_t^2)}{\hbar \omega} \coth(\beta\hbar\omega/2) \\
 &\equiv \frac{\hbar \rho c_t^2}{\pi \tilde{\gamma}^2 P_0 C_s} \frac{1}{\hbar \omega} \coth(\beta\hbar\omega/2). \quad (21)
 \end{aligned}$$

C. a mode

The antisymmetric modes have a more complicated asymptotic expansion. First, let us remark that for the lowest branch and any k_\parallel , both $\bar{k}_l = i\kappa_l$ and $\bar{k}_t = i\kappa_t$ take imaginary values, so we write Eq. (8b) in the form

$$\frac{\tanh(\kappa_l d/2)}{\tanh(\kappa_t d/2)} = \frac{4\kappa_t \kappa_l k_\parallel^2}{(\kappa_t^2 + \kappa_l^2)^2}. \quad (22)$$

Expanding this equation to the second leading order, we obtain a quadratic dispersion relation for very small k_\parallel ,⁹

$$\omega_{a,0,k_\parallel} = d c_t \sqrt{\frac{c_l^2 - c_t^2}{3c_l^2}} k_\parallel^2 \equiv \frac{\hbar}{2m^*} k_\parallel^2. \quad (23)$$

Nevertheless, this asymptotic expression is not enough for the calculation of $\langle |M_{a,0,k_\parallel}|^2 \rangle$, as it turns out that both expres-

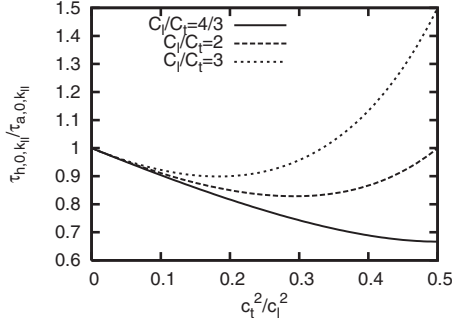


FIG. 2. The ratio $\tau_{h,0,k_{\parallel}(\omega)}/\tau_{a,0,k_{\parallel}(\omega)}$ as function of the ratio c_t^2/c_l^2 for different values of C_l/C_t . The value $C_l/C_t=4/3$ is the minimum possible value and, thus, all other curves lie above the solid curve in the plot.

sions (10c) and (14c) are zero in the first and second leading orders. Therefore, we have to expand to the third leading order to get nonzero results. From Eq. (8b), we obtain

$$\omega_{a,0,k_{\parallel}} = \frac{\hbar}{2m^*} \left(k_{\parallel}^2 - d^2 \frac{27c_l^2 - 20c_t^2}{90c_t^2} k_{\parallel}^4 \right), \quad (24)$$

from which we finally get

$$\begin{aligned} \tau_{a,0,k_{\parallel}(\omega)} &= \frac{\hbar \rho c_t^2}{\pi \tilde{\gamma}^2 P_0 C_l c_t^4 + C_t c_t^2 (c_l^2 - 2c_t^2)} \frac{\coth(\beta \hbar \omega / 2)}{\hbar \omega} \\ &= \frac{\hbar \rho c_t^2}{\pi \tilde{\gamma}^2 P_0 C_a} \frac{1}{\hbar \omega} \coth(\beta \hbar \omega / 2), \end{aligned} \quad (25)$$

with $C_a = 4C_s$.

D. Comparison of the scattering rates and mean free paths

The first thing to observe is that, although the dispersion relations for the s and a modes are different in the low k_{\parallel} limit, $\tau_{s,0,k_{\parallel}}$ and $\tau_{a,0,k_{\parallel}}$ are related by the simple equation $\tau_{s,0,\omega} = 4\tau_{a,0,\omega}$ (we shall simply write $\tau_{\sigma,0,\omega}$ for $\tau_{\sigma,0,k_{\parallel}(\omega)}$). In other words, the scattering rate for the s phonons is four times smaller than the scattering rate of a phonons at the same ω .

Let us now compare $\tau_{a,0,\omega}$ with $\tau_{h,0,\omega}$. For this, we calculate the ratio

$$\frac{\tau_{h,0,\omega}}{\tau_{a,0,\omega}} = \frac{C_l c_t^4 + C_t c_l^2 (c_l^2 - 2c_t^2)}{C_t c_l^2 (c_l^2 - c_t^2)} = 1 - (c_t/c_l)^2 \frac{1 - (C_l/C_t)(c_t/c_l)^2}{1 - (c_t/c_l)^2}. \quad (26)$$

In any normal material (i.e., with positive Poisson ratio), the ratio c_t^2/c_l^2 is restricted to $0 < c_t^2/c_l^2 \leq 1/2$, and for C_l/C_t , we have¹³ $C_l/C_t = 15/4\xi^2 - 10/\xi + 8 \geq 4/3$. In Fig. 2, we plot the ratio $\tau_{h,0,\omega}/\tau_{a,0,\omega}$ as function of c_t^2/c_l^2 for different values of C_l/C_t .

We first remark that in the limit $c_t/c_l \rightarrow 0$, $\tau_{h,0,\omega}/\tau_{a,0,\omega} = 1$, independent of the value for C_l/C_t . Increasing c_t/c_l will result in a decrease of $\tau_{h,0,\omega}/\tau_{a,0,\omega}$ until a minimum is reached at $(c_t/c_l)^2 = 1 - \sqrt{1 - (C_l/C_t)^{-1}}$, which lies between 0 and 1/2. Afterwards, $\tau_{h,0,\omega}/\tau_{a,0,\omega}$ increases monotonically until it

reaches the value $(C_l/C_t)/2$ for $(c_t/c_l)^2 = 1/2$. As $\tau_{h,0,\omega}/\tau_{a,0,\omega}$ increases monotonically with C_l/C_t , we conclude that $\tau_{h,0,\omega} < \tau_{a,0,\omega}$ for any c_t/c_l , as long as $C_l/C_t < 2$. For $C_l/C_t \geq 2$, $\tau_{h,0,\omega}$ can be either smaller or greater than $\tau_{a,0,\omega}$, depending on whether $(c_t/c_l)^2$ is smaller or greater than C_l/C_t , respectively. A typical value for $(c_t/c_l)^2$ in SiN_x is 0.36, which means that $\tau_{h,0,\omega} < \tau_{a,0,\omega}$ as long as C_l/C_t is smaller than 2.78.

When comparing $\tau_{s,0,\omega}$ with $\tau_{h,0,\omega}$, we encounter a similar situation. As $\tau_{s,0,\omega} = 4\tau_{a,0,\omega}$, the ratio $\tau_{h,0,\omega}/\tau_{s,0,\omega}$ has the same features as the ratio $\tau_{h,0,\omega}/\tau_{a,0,\omega}$, except for the fact that the critical value for C_l/C_t is 8, i.e., $\tau_{h,0,\omega}$ is always smaller than $\tau_{s,0,\omega}$ if $C_l/C_t < 8$ and can be either smaller or greater than $\tau_{s,0,\omega}$ for $C_l/C_t \geq 8$. For the SiN_x typical value, $(c_t/c_l)^2 = 0.36$, we have $\tau_{h,0,\omega} \leq \tau_{s,0,\omega}$ as long as $C_l/C_t \leq 17.6$.

More interesting than the scattering rates is to compare the phonon mean free paths, since these can be directly measured experimentally. For this, let us first use the dispersion relations (20) and (23), and $\omega_{h,0,k_{\parallel}} = c_t k_{\parallel}$ to write the expressions for the mean free paths:

$$l_{h,0,k_{\parallel}(\omega)} = c_t \tau_{h,0,k_{\parallel}} = \frac{\hbar \rho c_t^3}{\pi \tilde{\gamma}^2 P_0 C_t} \frac{1}{\hbar \omega} \coth(\beta \hbar \omega / 2) \quad (27a)$$

$$= \frac{\hbar \rho c_t^2}{\pi \tilde{\gamma}^2 P_0 C_t} \frac{1}{\hbar k_{\parallel}} \coth(\beta \hbar c_t k_{\parallel} / 2), \quad (27b)$$

$$l_{s,0,k_{\parallel}(\omega)} = c_s \tau_{s,0,k_{\parallel}} = \frac{\hbar \rho c_t^3}{\pi \tilde{\gamma}^2 P_0} \frac{2\sqrt{1 - c_t^2/c_l^2}}{C_s} \frac{\coth(\beta \hbar \omega / 2)}{\hbar \omega} \quad (28a)$$

$$= \frac{\hbar \rho c_t^2}{\pi \tilde{\gamma}^2 P_0 C_s} \frac{1}{\hbar k_{\parallel}} \coth(\beta \hbar c_s k_{\parallel} / 2), \quad (28b)$$

$$\begin{aligned} l_{a,0,k_{\parallel}(\omega)} &= \sqrt{\frac{2\hbar\omega}{m^*}} \tau_{a,0,k_{\parallel}} \\ &= \frac{\hbar \rho c_t^3}{\pi \tilde{\gamma}^2 P_0} \frac{2(1 - c_t^2/c_l^2)^{1/4}}{3^{1/4} C_a} \sqrt{\frac{d\omega}{c_t}} \frac{\coth(\beta \hbar \omega / 2)}{\hbar \omega} \end{aligned} \quad (29a)$$

$$= \frac{\hbar \rho c_t^2}{\pi \tilde{\gamma}^2 P_0 C_a} \frac{2}{\hbar k_{\parallel}} \coth\left(\frac{\beta \hbar d c_t}{2\sqrt{3}} \sqrt{1 - c_t^2/c_l^2} k_{\parallel}\right). \quad (29b)$$

A way to determine the mean free path of phonons is to measure the resonant attenuation of ultrasound propagating along the membrane. If this is experimentally impossible, another way to determine the material parameters is to make acoustic measurements on thicker and wider membranes. Note, however, that elastic waves attenuate not only because of resonant scattering of phonons [Eqs. (27)–(29)], but also due to energy relaxation.¹⁴ Nevertheless, since we are interested here in the thermal properties of the membranes, only the resonant scattering is important and we disregard the energy relaxation mechanism.

To analyze the results (27)–(29) in more detail, we expressed the mean free paths both in terms of the angular frequency and in terms of k_{\parallel} . If the elastic modes of different polarizations are produced with the same ω , then we should compare the mean free paths as given by the expressions (27a), (28a), and (29a), which we denote as $l_{\sigma,0,\omega}$. For example, $l_{h,0,\omega}/l_{s,0,\omega} = (\tau_{h,0,\omega}/\tau_{s,0,\omega})(c_t/c_s)$, which is smaller than $(\tau_{h,0,\omega}/\tau_{s,0,\omega})$ in any material. The discussion we made above about $\tau_{h,0,\omega}/\tau_{s,0,\omega}$ applies here too.

The expressions (29) for $l_{a,0,\omega}$ are very different from the ones for $l_{h,0,\omega}$ and $l_{s,0,\omega}$. Nevertheless, the expressions (27)–(29) are calculated for $k_{\parallel} \ll 1/d$, which means that $\omega d \ll (2\pi/k_{\parallel})\omega = c_t$, which implies $\sqrt{\omega d}/c_t \ll 1$. Taking this into account when we compare the expressions for $l_{h,0,\omega}$, $l_{s,0,\omega}$, and $l_{a,0,\omega}$, at the same ω , we conclude that, as a function of frequency, for low enough frequencies the antisymmetric Lamb modes have the shortest mean free path. This is a consequence of the fact that the group velocity of the a modes decreases to zero as k_{\parallel} decreases.

If we compare $l_{h,0,k_{\parallel}}$ and $l_{s,0,k_{\parallel}}$ as functions of k_{\parallel} , we see that $l_{h,0,k_{\parallel}}/l_{s,0,k_{\parallel}} = (\tau_{h,0,k_{\parallel}}/\tau_{s,0,k_{\parallel}})[\coth(\beta\hbar c_t k_{\parallel}/2)/\coth(\beta\hbar c_s k_{\parallel}/2)]$, which is bigger than $\tau_{h,0,k_{\parallel}}/\tau_{s,0,k_{\parallel}}$, since $c_t < c_s$ implies $\coth(\beta\hbar c_t k_{\parallel}/2) > \coth(\beta\hbar c_s k_{\parallel}/2)$. Comparing $l_{a,0,k_{\parallel}}$ with expressions (27b) and (28b), we observe, for example, that both $l_{a,0,k_{\parallel}}/l_{h,0,k_{\parallel}}$ and $l_{a,0,k_{\parallel}}/l_{s,0,k_{\parallel}}$ are proportional to $\coth(\beta\hbar\omega_{a,0,k_{\parallel}}/2)/\coth(\beta\hbar\omega_{h/s,0,k_{\parallel}}/2)$. However, again, for long wavelengths, due to the quadratic dependence of $\omega_{a,0,k_{\parallel}}$ on k_{\parallel} , we have $\omega_{a,0,k_{\parallel}} \ll \omega_{h/s,0,k_{\parallel}}$. Moreover, $\coth(x) \sim 1/x$ for $x \rightarrow 0$, so both $l_{a,0,k_{\parallel}}/l_{h,0,k_{\parallel}}$ and $l_{a,0,k_{\parallel}}/l_{s,0,k_{\parallel}}$ are proportional to $1/k_{\parallel}$ and become very big in the limit of long wavelengths. In conclusion, as function of k_{\parallel} in the limit $dk_{\parallel} \ll 1$, the antisymmetric modes have a much longer mean free path than the symmetric and horizontal shear modes with the same k_{\parallel} .

E. Calculation of the heat conductivity

Now we calculate the heat conductivity in the limit of low temperature. In that limit, only the lowest branch of each polarization will be populated. Furthermore, in the low temperature range that we are interested in (typical temperatures are below 300 mK), the typical phonon frequency cutoff in amorphous materials can be neglected. In the \mathbf{k}_{\parallel} space, the density of states is $A/(2\pi)^2$ and, after some changes of variables, we write Eq. (17) in the form

$$\kappa = \frac{\hbar^2}{16\pi k_B T^2} \sum_{\sigma} \int_{\omega_{\sigma,0}}^{\infty} d\omega \frac{k_{\parallel,\sigma,0}(\omega) l_{\sigma,0,k_{\parallel}} \omega^2}{\sinh^2(\beta\hbar\omega/2)}, \quad (30)$$

where the lower limits $\omega_{\sigma,0}^*$ were introduced for the reasons that will become clear immediately. Using Eqs. (27)–(29) for the mean free paths, we express κ as a sum of three contributions:

$$\kappa = \frac{k_B^2 \rho c_t^2}{16\pi^2 \hbar \tilde{\gamma}^2 P_0} T \left(\frac{I(x_{h,0}^*)}{C_t} + \frac{I(x_{s,0}^*)}{C_s} + \frac{2I(x_{a,0}^*)}{C_a} \right), \quad (31)$$

where $x_{\sigma,0}^* \equiv \beta\hbar\omega_{\sigma,0}^*$ and by $I(x)$ we denoted the integral

$$I(x) \equiv \int_x^{\infty} dy \frac{y^2 \coth(y/2)}{\sinh^2(y/2)} = \frac{4x^2 e^x}{(e^x - 1)^2} + \frac{8x}{e^x - 1} - 8 \ln(1 - e^{-x}). \quad (32)$$

Note that, although the mean free paths for the h and s modes have different functional dependencies on ω than the mean free path for the a modes, the integrand in Eq. (31) is the same for all three modes. The role of the lower cutoff in Eq. (30) becomes obvious when we look at Eq. (32): the integral $I(x)$ has a logarithmic divergence in $x=0$.

If the cutoff is small enough, then we can approximate $I(x)$ by

$$I(x) \approx 12 - 8 \ln(x), \quad (33)$$

and inserting this into Eq. (31), we obtain

$$\kappa = \frac{k_B^2 \rho c_t^2}{4\pi^2 \hbar \tilde{\gamma}^2 P_0} T \left[\frac{3 - 2 \ln(\beta\hbar\omega_{h,0}^*)}{C_t} + \frac{3 - 2 \ln(\beta\hbar\omega_{s,0}^*)}{C_s} + \frac{2[3 - 2 \ln(\beta\hbar\omega_{a,0}^*)]}{C_a} \right], \quad (34)$$

where the first, second, and third terms in the square brackets above give the contributions of the h , s , and a phonon modes to the heat conductivity. The above expression leads to the temperature dependence $\kappa \propto T(a + b \ln T)$ and this dependence is a hallmark of the TLS-limited heat conductance at low temperature.

For a numerical estimate, let us use for the cutoff the finite size of the membrane, which limits the wave vectors to values of the order of $2\pi/\sqrt{A}$. For the typical experimental parameters $T=0.1$ K, $\sqrt{A}=400$ μm , and $d=200$ nm,^{1,2,7} we have $\ln(x_{h,0,2\pi/L}) \approx -4.9$, $\ln(x_{s,0,2\pi/L}) \approx -4.4$, and $\ln(x_{a,0,2\pi/L}) \approx -11.4$. However, since $C_a=4C_s$ [see Eqs. (21) and (25)], the contributions of all the phonon polarizations to the heat conductivity are of the same order.

V. CONCLUSIONS

We used the model introduced in Ref. 13 to calculate the scattering of the elastic modes in a thin, amorphous membrane. We modeled the scattering centers in the membrane by an ensemble of TLSs with the same properties and distribution over energy splitting and asymmetry as the TLSs in a bulk material. Whether this assumption is valid remains to be checked by experiment. We obtained the expressions for the TLS relaxation time [Eq. (15)], for the phonon scattering time [Eq. (16)], and for the heat conductivity κ [Eq. (17)].

For general temperatures, the heat conductivity and the scattering times have to be calculated numerically. We calculated analytical low temperature approximations and compared the mean free paths of different phonon polarizations. In this way, we observed that the contribution of the lowest branches of the phonon modes to the heat conductivity are logarithmically divergent at $k_{\parallel} \rightarrow 0$. This could be a reason for which in some experiments a radiative heat transport is observed.⁵ Nevertheless, there is a natural lower cutoff of $k_{\parallel} \rightarrow 0$ due to the finite size of the membrane. This cutoff renders κ finite, which, in the low temperature limit, behaves

like $\kappa \propto T(a+b \ln T)$. This behavior is a hallmark of the TLS-limited heat conductance at low temperature.

Due to the dispersion relations of the phonon modes, the TLS distribution in the low energy limit has a bigger impact on the heat conductivity in thin membranes than in bulk materials. If we, for instance, modify the distribution (3) into

$$P'(\epsilon, u) = \frac{P_0}{\epsilon^\alpha u \sqrt{1-u^2}},$$

with an extra energy dependence $\epsilon^{-\alpha}$, we make the expression (30) for κ convergent even in the $\omega_{\alpha,0}^* \rightarrow 0$ limit, which leads to a low temperature asymptotic dependence of κ

$\propto T^{1+\alpha}$. However, whether this is the situation or not has to be decided experimentally.

ACKNOWLEDGMENTS

Discussions with J. P. Pekola, I. J. Maasilta, and V. Vinokur are gratefully acknowledged. This work was partly supported by the U.S. Department of Energy, Office of Science, under Contract No. DE-AC02-06CH11357 and by the NATO Grant No. EAP.RIG 982080. D.V.A. acknowledges the hospitality of the University of Jyväskylä, where part of this work has been carried out, and the financial support from the Academy of Finland.

-
- ¹M. Leivo, Ph. D. thesis, University of Jyväskylä, 1999.
²M. M. Leivo and J. P. Pekola, *Appl. Phys. Lett.* **72**, 1305 (1998).
³W. Holmes, J. M. Gildemeister, P. L. Richards, and V. Kotsubo, *Appl. Phys. Lett.* **72**, 2250 (1998).
⁴A. L. Woodcraft, R. V. Sudiwalaa, E. Wakui, R. S. Bhatia, J. J. Bock, and A. D. Turner, *Physica B* **284**, 1968 (2000).
⁵H. F. C. Hoevers, M. L. Ridder, A. Germeau, M. P. Bruijn, P. A. J. de Korte, and R. J. Wiegink, *Appl. Phys. Lett.* **86**, 251903 (pages 3) (2005).
⁶B. L. Zink and F. Hellman, *Solid State Commun.* **129**, 199 (2004).
⁷D. V. Anghel, J. P. Pekola, M. M. Leivo, J. K. Suoknuuti, and M. Manninen, *Phys. Rev. Lett.* **81**, 2958 (1998).
⁸B. A. Auld, *Acoustic Fields and Waves in Solids*, 2nd ed. (Krieger, Melbourne, FL, 1990).
⁹T. Kühn, D. V. Anghel, J. P. Pekola, M. Manninen, and Y. M. Galperin, *Phys. Rev. B* **70**, 125425 (2004).
¹⁰P. W. Anderson, B. I. Halperin, and C. M. Varma, *Philos. Mag.* **25**, 1 (1972).
¹¹W. A. Phillips, *J. Low Temp. Phys.* **7**, 351 (1972).
¹²P. Esquinazi, *Tunneling Systems in Amorphous and Crystalline Solids* (Springer, New York, 1998).
¹³D. V. Anghel, T. Kühn, Y. M. Galperin, and M. Manninen, *Phys. Rev. B* **75**, 064202 (2007).
¹⁴J. Jäckle, *Z. Phys.* **257**, 212 (1972).
¹⁵A. J. Leggett, S. Chakravarty, A. T. Dorsey, M. P. A. Fisher, A. Garg, and W. Zwerger, *Rev. Mod. Phys.* **59**, 1 (1987).
¹⁶D. V. Anghel and T. Kühn, *J. Phys. A* **40**, 10429 (2007).